

# Development of an infrared spectroscopic approach for studying metalloenzyme active site chemistry under direct electrochemical control

Adam J. Healy, Holly A. Reeve and Kylie A. Vincent\*

Received 15th March 2010, Accepted 9th April 2010

DOI: 10.1039/c004274a

Direct electrochemical methods have been productive in revealing mechanistic details of catalysis by a range of metalloenzymes including hydrogenases and carbon and nitrogen cycling enzymes. In this approach, termed protein film electrochemistry, the protein is attached or adsorbed on the electrode surface and exchanges electrons directly, providing precise control over redox states or catalysis and avoiding diffusion-limited electron transfer. The 'edge' surface of pyrolytic graphite has proved to be a particularly good surface for adsorption of proteins in electroactive conformations. We now describe development of an approach that combines the precise control achieved in direct electrochemical measurements at a graphite electrode with surface infrared (IR) spectroscopic analysis of chemistry occurring at metallocentres in proteins. Hydrogenases are of particular interest: their unusual organo-metallic active sites – iron or nickel-iron centres coordinated by CO and CN<sup>−</sup> – give rise to IR  $\nu(\text{CO})$  and  $\nu(\text{CN})$  bands that are detected readily because these ligands are strong vibrational oscillators and are sensitive to changes in electron density and coordination at the metals. Small diatomic species also bind as exogenous ligands (as substrate, product, activator or inhibitor) to a range of other important metalloproteins, and understanding their reactivity and binding selectivity is critical in building up a multidimensional picture of enzyme chemistry and evolutionary history. The surface IR spectroelectrochemical approach we describe is based around Attenuated Total Reflectance (ATR) mode sampling of a film of pyrolytic graphite particles modified with a protein of interest. The particle network extends the electrode into three-dimensional space, providing sufficient adsorbed protein for spectroscopic analysis under precise electrochemical control. This strategy should open up new opportunities for detection of redox-dependent chemistry at metal centres in proteins, including short-lived catalytic intermediates and time-resolved details of catalysis and inhibition.

## Introduction

Metalloenzymes catalyse a series of redox reactions relevant to energy cycling technologies, and there is significant interest in taking lessons from nature for development of selective future energy-cycling catalysts based around readily available metals.<sup>1,2</sup> In energy catalysis, IR spectroscopic techniques addressing precious metal surfaces have played a significant role in elucidating catalytic mechanisms, intermediates and catalyst poisoning pathways because a number of the players in these

*Inorganic Chemistry Laboratory, Department of Chemistry, University of Oxford, South Parks Road, Oxford, OX1 3QR, UK. E-mail: kylie.vincent@chem.ox.ac.uk*

pathways are small molecules, such as CO and CO<sub>2</sub>, which give rise to strong IR-active vibrational bands which are sensitive to electron density at the metal. In particular, *in situ* spectroelectrochemical approaches, in which IR sampling is combined with electrochemical control, have been instructive in revealing potential dependent details of electrocatalysis.<sup>3–5</sup>

Catalysis by the [NiFe] and [FeFe] hydrogenases has attracted particular interest because H<sub>2</sub> oxidation and production occur at high turnover frequencies and at minimal overpotential, close to  $E(2\text{H}^+/\text{H}_2)$ .<sup>6</sup> Cycling of hydrogen in the presence of O<sub>2</sub> by certain hydrogenases leads to possibilities for consumption of H<sub>2</sub> from fuel/oxidant mixtures, or photo-biological generation of H<sub>2</sub> in the presence of O<sub>2</sub> from water splitting.<sup>7</sup> Certain hydrogenases also exhibit substantial insensitivity to CO or sulfides which poison precious metal surfaces.<sup>6</sup> The attraction of cycling hydrogen at catalytic centres comprising common metals (Fig. 1A) has led to synthesis of a wide range of related transition metal carbonyl clusters possessing structural similarity to hydrogenases with the aim of mimicking reactivity of the enzymes.<sup>1</sup> For these small molecule systems, *in situ* spectroelectrochemical approaches targeting  $\nu(\text{CO})$  or  $\nu(\text{CN})$  vibrational bands have been exploited to identify short-lived intermediates, diagnose redox-coupled structural changes and monitor side reactions.<sup>8–10</sup> These studies have been carried out largely in an external reflection-absorption spectroscopic configuration in which a thin solution layer (*ca* 20  $\mu\text{m}$ ) of sample is trapped between an IR transparent window and a mirror-polished gold or carbon working electrode.<sup>8</sup>

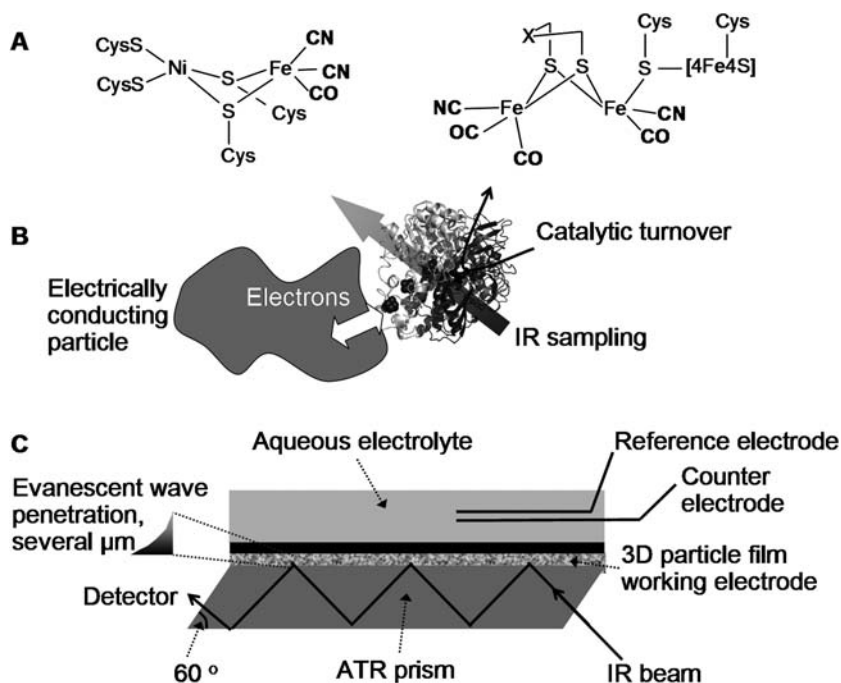


**Fig. 1** (A) The active sites of (left) [NiFe]- and (right) [FeFe]-hydrogenases incorporate CO and CN<sup>−</sup> as integral ligands, and these provide a useful IR spectroscopic handle for studying active site chemistry. (B) An IR spectroelectrochemical approach for studying redox enzymes, based on the concept of direct electron transfer between the protein and an electrically conducting particle. (C) Schematic representation of an Attenuated Total Reflectance (ATR) IR approach for studying immobilised enzyme under direct electrochemical control: the cell comprises a silicon parallelogram prism coated with a thin film (ideally *ca* 5  $\mu\text{m}$  thick) of enzyme-modified pyrolytic graphite particles in Nafion-phosphate.

Solution IR spectroelectrochemical approaches have also been employed widely to study potential-dependent changes in the  $\nu(\text{CO})$  or  $\nu(\text{CN})$  bands associated with hydrogenase active site ligands, Fig. 1A.<sup>11</sup> Enzyme molecules are generally too large for efficient diffusion and electrochemical control is either very slow or indirect and dependent on dissolved redox mediators. These studies generally employ a transmission cell incorporating a partially transparent gold-minigrid electrode, and have revealed a range of active and inactive states for hydrogenases, contributing to our understanding of the mechanisms of these enzymes and highlighting subtle differences between the conditions for generation of certain states for enzymes from different organisms. Mediated spectroelectrochemistry for redox proteins has also been carried out in an internal Attenuated Total Reflectance (ATR) IR configuration.<sup>12</sup>

More precise control over the redox states of hydrogenases is achieved in protein film electrochemistry in which a submonolayer film of enzyme is adsorbed on an electrode surface in direct electronic communication with the electrode.<sup>6</sup> The fast, direct electron transfer achieved in protein film electrochemistry is particularly valuable during rapid catalytic turnover when mediated electron transfer quickly becomes limited by mediator diffusion.<sup>13</sup> Experiments of this type have identified states of hydrogenases that depend critically on electrode potential, such as a sulfide-inhibited form of [NiFe] hydrogenase that is stable only in a narrow potential window.<sup>14</sup> The products of  $\text{O}_2$  inactivation of hydrogenases and the ability of some hydrogenases to recover easily from  $\text{O}_2$  attack are important questions in understanding catalytic selectivity; these reactions appear to be modulated by subtle differences in the thermodynamics and kinetics of redox-linked reactions in the enzymes.<sup>6,15,16</sup> For hydrogenases and other metalloenzymes that bind small molecule ligands, there is a need for *in situ* surface spectroelectrochemical approaches for addressing active site chemistry under the direct control of an electrode.

The large footprint of proteins on a surface (*ca* 20 nm<sup>2</sup> for many [NiFe]-hydrogenases) limits coverage to a few pmol cm<sup>-2</sup>, imposing significant technical challenges for IR spectroscopic sampling of sub-monolayer films on a planar electrode. One solution to the sensitivity challenge has been to exploit a surface enhancement of the IR signal that occurs in regions close to a nanoscale roughened metal surface (strongest within a few nanometres). Surface Enhanced Infrared Absorption (SEIRA) spectroelectrochemistry in an ATR-IR configuration has been demonstrated in several studies of potential-dependent changes in the amide spectral region for cytochrome *c* immobilised on a self-assembled monolayer on a thin film gold electrode deposited on an ATR prism.<sup>17,18</sup> For hydrogenases, obtaining sustained electrocatalytic activity on gold electrodes has proved difficult, although there have been several very promising reports of SEIRA spectroscopy applied to hydrogenases on gold.<sup>19,20</sup> Carbon, specifically the 'edge' surface of pyrolytic graphite, has been the electrode material of choice for protein film electrochemical studies of hydrogenases<sup>6</sup> and a wide range of other proteins.<sup>13,21,22</sup> We have therefore sought an *in situ* surface spectroelectrochemical method suitable for application to protein films on pyrolytic graphite.

The surface IR spectroelectrochemical strategy we describe here relies upon protein immobilised on a high surface-area, three-dimensional electrode. Pyrolytic graphite is easily sanded into plate-like particles with a mean particle flat surface area of about 11  $\mu\text{m}^2$ .<sup>23</sup> By analogy with the surfaces of bulk graphite, the 'edge' surface should be excellent for adsorption of hydrogenases and other proteins in suitable orientations for fast electron transfer (Fig. 1B). This is confirmed by demonstrations that graphite particles can connect pairs of redox enzymes which then engage in oxidative and reductive catalysis, including nitrate reduction to nitrite by  $\text{H}_2$  on particles modified with hydrogenase and nitrate reductase,<sup>23</sup> and the water-gas shift reaction, converting CO and water to  $\text{CO}_2$  and  $\text{H}_2$  catalysed by particles modified with hydrogenase and carbon monoxide dehydrogenase.<sup>24</sup> In the IR surface spectroelectrochemical approach under development in our laboratory, we

now make use of graphite particles modified with a single protein of interest to assemble a high surface-area electrode for IR spectroscopic study under electrochemical control. As a binder, we exploit an aqueous suspension of the polymer electrolyte Nafion, titrated to neutral pH with solutions of sodium hydroxide and sodium dihydrogen phosphate. The Nafion-phosphate dries to leave a biocompatible hydrated polymer network in which proton transport is efficient – particularly important for hydrogenases for which protons are the substrate/product. A similar approach is used to bind metal nanoparticle-loaded carbon black particles in Nafion for fuel cell electrodes.<sup>25</sup> Networks of conducting particles have also been exploited as high surface area electrodes for enzyme electrocatalysis in fuel cells, for example, electrocatalytic fructose oxidation by fructose dehydrogenase adsorbed onto a network of Ketjen black nanoparticles bound with poly(vinylidene difluoride) onto carbon paper.<sup>26</sup>

For a spectroscopic experiment, the Nafion-phosphate film of particles is coated onto the ATR prism such that the evanescent wave from the internally reflected IR beam penetrates *ca* 5  $\mu\text{m}$  beyond the prism into the film (Fig. 1C). An electrochemical cell is then assembled on top of the prism, incorporating counter and reference electrodes in aqueous buffered electrolyte, and fittings for gas access. The hydrated polymer electrolyte may actually bear some similarity to the environment of proteins in the native viscous cellular matrix. An added advantage of working in Nafion-phosphate is a reduction in intensity of vibrational bands arising from the solvent water, and water is further excluded by incorporation of solid particles into films. Strong IR absorption by water in the 3600–3000 and 1700–1600  $\text{cm}^{-1}$  regions, and weaker absorption in the 2300–2000  $\text{cm}^{-1}$  region can otherwise present serious challenges for IR spectroscopic study of bio-molecules. In principle, however, with some modifications to the cell, particles could be pressed between the prism and a conducting backing plate in water without Nafion-phosphate as binder.

We demonstrate that a particle film assembled in Nafion-phosphate provides high quality spectra for CO bound at the heme centre of myoglobin, and functions as a viable electrode for electrocatalysis by hydrogenase and spectroelectrochemical cycling of  $[\text{Fe}(\text{CN})_6]^{3-/4-}$  trapped within a particle film. These developments set the scene for application of the approach to a range of hydrogenase enzymes as well as other metalloproteins bearing ligands with IR-active vibrations such as CO, NO,  $\text{CO}_2$  or  $\text{SCN}^-$ . We hope that this approach will provide significant insight into potential-dependent reactions of these systems.

## Methods

### Preparation of films

Tris-HCl buffer (50 mM, pH 8) was prepared from Trizma base (Sigma) titrated with HCl (BDH), and phosphate buffers (50 mM, pH 7) were prepared from  $\text{Na}_2\text{HPO}_4$  and  $\text{NaH}_2\text{PO}_4$  (BDH), using MilliQ water, resistivity 18  $\text{M}\Omega\text{ cm}$ . Nafion perfluorinated ion-exchange resin (10% dispersion in water, Aldrich, pH < 2) was titrated to a slightly basic pH with concentrated NaOH (BDH) and then back to pH 7 with a solution of  $\text{NaH}_2\text{PO}_4$  (*ca* 0.5 M) to give Nafion-phosphate as a *ca* 8% aqueous dispersion. An ATR-IR spectrum of Nafion-phosphate was obtained by depositing 2  $\mu\text{L}$  of the dispersion, diluted 1 : 1 with phosphate buffer (pH 7, 50 mM), onto the silicon ATR prism over an area approximately  $4 \times 6\text{ mm}^2$ . Particles of pyrolytic graphite were prepared freshly by abrading an ‘edge’ surface of pyrolytic graphite (Momentive Performance Materials) with sandpaper (P800 grade, Norton Abrasives).

Equine skeletal myoglobin (Sigma) was dissolved in phosphate buffer to give a 4 mM stock solution. In an anaerobic glove box (mBraun,  $\text{O}_2 < 0.1\text{ ppm}$ ), myoglobin was reduced with excess sodium dithionite (BDH), which was then removed using a 3000 molecular weight cutoff centrifugal filter device (Millipore Microcon Ultracel YM-3) by repeated washing with phosphate buffer until the

filtrate was no longer reducing to methyl viologen. Under red light, a 20  $\mu\text{L}$  aliquot of *ca* 4 mM reduced myoglobin was injected *via* a septum into a vial flushed with CO (BOC) and containing 20  $\mu\text{L}$  of *ca* 8% aqueous Nafion-phosphate dispersion. The vial was allowed to stand in the dark for 30 min at 20  $^{\circ}\text{C}$ , and then 2  $\mu\text{L}$  of the mixture (containing *ca* 4 nmoles of myoglobin) was removed and deposited on a silicon ATR prism, also over an area approximately  $4 \times 6 \text{ mm}^2$ , and allowed to dry for 5 min to give a partially hydrated polymer electrolyte film of carboxymyoglobin for IR spectroscopic study. The gas-tight ATR cell was assembled and sealed over the prism in the glove box under red light. The cell is non-transparent to visible light, preventing photolysis of CO during transport to the FTIR sample compartment. A second film incorporating pyrolytic graphite particles was prepared by dispersion of freshly sanded particles into the Nafion-phosphate carboxy-myoglobin mixture and depositing this onto the ATR prism in a similar manner.

*Escherichia (E.) coli* hydrogenase 1 was purified according to a published procedure and concentrated to *ca* 1  $\text{mg mL}^{-1}$ .<sup>15</sup> Electrochemical measurements on hydrogenase were performed in an anaerobic glove box (mBraun, <0.1 ppm  $\text{O}_2$ ) using a pyrolytic graphite 'edge' (PGE) rotating disc electrode (RDE) with planar surface area 0.03  $\text{cm}^2$ . The electrode was cleaned by polishing with an aqueous slurry of  $\alpha$ -alumina (1  $\mu\text{m}$ , Buehler), washing in aqua regia, followed by rinsing and sonication. A film of hydrogenase was prepared by freshly abrading the electrode surface with P800 sandpaper, sonicating for 10 s in MilliQ water, rinsing, shaking off excess water, and then spotting on 0.5  $\mu\text{L}$  of hydrogenase and allowing 5 min for the protein to adsorb. The electrode was then immersed in enzyme-free Tris-HCl buffer solution flushed with  $\text{H}_2$  (Air Products, Premier Plus) for electrochemical measurements. Films of hydrogenase were first activated at  $-0.558 \text{ mV}$  for 600 s in  $\text{H}_2$ -saturated solution before cycling the potential. To apply a Nafion-phosphate overlayer, the hydrogenase-modified electrode was removed from solution, shaken to remove excess buffer, and coated with Nafion-phosphate diluted to a *ca* 1% suspension with Tris-HCl buffer. The Nafion-phosphate layer was then allowed to dry for 5 min before re-immersing the electrode in buffered electrolyte.

To prepare a hydrogenase-loaded particle film, freshly prepared pyrolytic graphite particles (*ca* 4 mg) were first sonicated for 10 s in Tris-HCl buffer followed by addition of hydrogenase (1  $\mu\text{L}$ ). The suspension was left for 5 min to allow hydrogenase to adsorb on the surface of the particles, and then centrifuged for 5 min (2000 G) to enable excess liquid to be removed. Particles were then washed with 10  $\mu\text{L}$  Tris-HCl buffer to remove unbound hydrogenase, separated again by centrifugation, and mixed with *ca* 1% Nafion-phosphate (*ca* 2.5  $\mu\text{L}$ ). A 0.5  $\mu\text{L}$  aliquot of this particle suspension was then spotted onto a freshly sanded PGE RDE and allowed to dry for 5 min before immersion in the buffered electrolyte.

A stock solution of 6 mM potassium ferricyanide (Aldrich, ACS) was prepared in water. A film incorporating pyrolytic graphite particles and ferricyanide (1 nmole) in Nafion-phosphate was deposited on the silicon ATR prism and left in air for 5 min to achieve partial drying. A piece of carbon paper (LT-1200N Gas Diffusion Layer, non-woven configuration, E-Tek) was pressed onto the film and the ATR cell, incorporating electrode connections as described below, was assembled over the prism.

### Electrochemical and infrared spectroscopic measurements

Infrared spectroscopic measurements were carried out using a Bio-Rad FTS-6000 FTIR spectrometer controlled by Digilab Resolutions Pro 4.0 software. The instrument was equipped with a liquid nitrogen-cooled Mercury Cadmium Telluride (MCT) detector and ATR accessory (Thermo Spectra-Tech) comprising a set of gold-plated mirrors which direct the IR beam *via* a series of internal reflections in the silicon ATR prism to the detector. The sample compartment was purged with dry nitrogen. Electrochemical experiments were performed using an EcoChemie Autolab PGSTAT 128N equipped with a sensitive electrochemical detection

module, and for spectroelectrochemical measurements a VersaSTAT 3 potentiostat (Ametek) provided potential control.

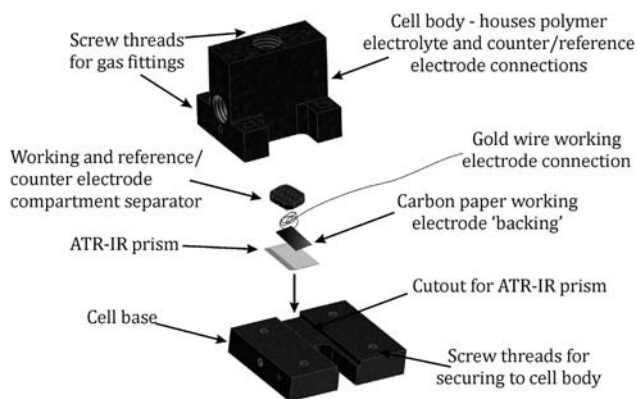
### Attenuated total reflectance IR spectroelectrochemical cell

A IR spectroelectrochemical cell for studying enzyme-modified graphite particle films in ATR mode was machined from PEEK to house a silicon parallelogram ATR prism ( $10 \times 5 \times 1 \text{ mm}^3$ , angle  $60^\circ$ , Crystal GmbH) polished on four optical faces, as shown in Fig. 2. The cell base comprises a groove to support the prism, and pins for location of the cell on a platform inside the FTIR sample compartment. A sheet of carbon paper inserted above the prism provides electrochemical contact across the film of particles coated on the prism. Mechanical contact with a coiled gold wire (Alfa Aesar, 0.127 mm diameter) provides electrical connection to the carbon paper. A PEEK divider with an array of *ca* 0.05 mm diameter holes drilled across the surface provides electrolyte contact between the working electrode and the reference and counter electrode compartment. A platinum wire counter electrode, and silver wire pseudo reference electrode (both Alfa Aesar, 0.127 mm diameter) are inserted through a screw fitting sealed with an o-ring into the cell body. Further screw fittings were sealed with PEEK plugs, but can also be used to connect gas inlet and outlet tubes into the cell body for studies in which gas control is required. A piece of damp tissue was placed in a cavity inside the cell wall to maintain a constant level of humidity in the cell after preparing each partially dried Nafion-phosphate film.

## Results and discussion

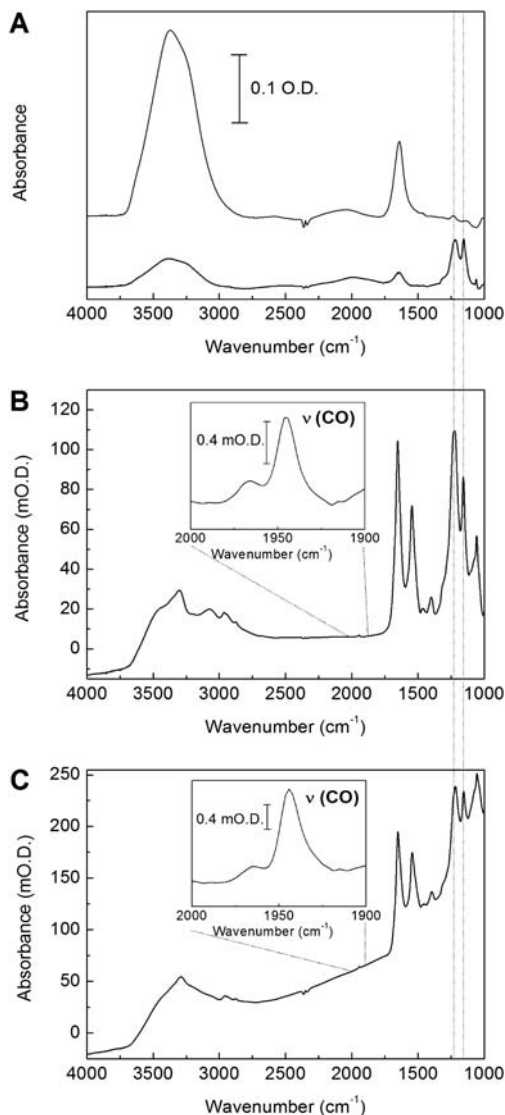
### Attenuated total reflectance IR spectroscopy for protein particle films

Fig. 3A compares the ATR-IR spectrum for a partially dried (5 min) Nafion-phosphate film (black) with a spectrum recorded when the ATR cell is filled with water (grey). Both spectra are processed against a spectrum of the empty cell (ie with the prism unmodified). Intense water absorption bands at *ca* 3600–3000 and 1700–1600  $\text{cm}^{-1}$  diminish in intensity as the Nafion-phosphate film dries, but are still clearly apparent after 5 min of drying, indicating that water is retained in the polymer structure. A constant level of humidity in the cell was ensured by including a piece of wet tissue in the sealed cell during all measurements. Nafion-phosphate gives rise to fairly sharp absorption bands below 1250  $\text{cm}^{-1}$ .<sup>27</sup>



**Fig. 2** Lift-out diagram of the ATR spectroelectrochemical cell used in this work, prepared using Computer Aided Design (CAD).





**Fig. 3** Spectra recorded in the ATR-IR cell. Each spectrum represents an average of 1000 co-added scans recorded at a resolution of  $4\text{ cm}^{-1}$  and is processed against a background of the cell with an unmodified prism. Panel A: Cell filled with water (grey, upper trace) or with a film of partially hydrated Nafion-phosphate on the silicon prism (black, lower trace). Panel B: Film of reduced CO-exposed myoglobin (4 nmoles) in Nafion-phosphate. Panel C: As for (B) but with pyrolytic graphite particles included in the film. The inset in panels B and C is an expansion of the region of the spectrum showing CO bound to the heme centre of myoglobin. A linear baseline correction was applied to the  $\nu(\text{CO})$  region of the spectrum shown in Figure 3C inset. Spectral features below  $1250\text{ cm}^{-1}$  due to Nafion-phosphate are indicated by grey dotted vertical lines.

Fig. 3B shows an ATR-IR spectrum of reduced equine skeletal myoglobin exposed to CO in a Nafion-phosphate film, processed against a spectrum of the empty ATR cell. The Amide I and II bands of the protein centred at about  $1650$  and  $1545\text{ cm}^{-1}$  are clearly visible. Since the Nafion-phosphate film had been previously stored in a vial flushed with dry CO, the film holds less water than the film of Nafion-phosphate film (panel A), and the  $2600\text{--}1750\text{ cm}^{-1}$  region of the spectrum

is essentially clear of solvent vibrational bands. The  $\nu(\text{CO})$  stretching bands associated with CO at the heme centre are just visible in the full spectrum. Note that no baseline correction or further spectral processing was necessary. The  $\nu(\text{CO})$  stretching bands are presented more clearly in the expanded trace in the inset to Fig. 3B. Just 4 nmoles of myoglobin were present in the film. The correspondence of the  $\nu(\text{CO})$  band positions, 1966 and 1945  $\text{cm}^{-1}$  to those expected for the  $A_0$  and  $A_1$  bands of carbonmonoxymyoglobin<sup>28</sup> is consistent with the protein remaining in a native-like conformation in the polymer electrolyte film. Spectra were unchanged for samples of carbonmonoxymyoglobin in Nafion-phosphate left at 20 °C in the dark under anaerobic conditions over a period of at least 6 h, indicating that the protein has good long-term stability in the hydrated polymer environment.

Fig. 3C shows that inclusion of pyrolytic graphite particles in a film of CO-exposed myoglobin, and addition of a carbon paper backing plate, have negligible effect on the quality of the spectral response. It is therefore possible to obtain informative spectra of proteins incorporated in a high-surface area graphite particle electrode at achievable protein loadings (at the level of several nmoles).

### Electrocatalysis by a hydrogenase in Nafion-phosphate films

Fig. 4 shows results which demonstrate that the electrocatalytic activity of a hydrogenase film on a graphite electrode is retained in contact with a Nafion-phosphate overlayer, and on a high surface area electrode constructed from a network of graphite particles in Nafion-phosphate. The response at an unmodified pyrolytic graphite 'edge' (PGE) rotating disk electrode (RDE) is shown in trace (i). Traces labelled (ii) in Fig. 4 are cyclic voltammograms recorded for a film of *E. coli* [NiFe] hydrogenase 1 adsorbed on the PGE RDE. The electrode is immersed in enzyme-free electrolyte (Tris-HCl, pH 8) flushed with  $\text{H}_2$  at 20 °C, and is rotated rapidly to ensure efficient supply of substrate and removal of product. Electrocatalytic  $\text{H}_2$  oxidation commences at *ca*  $-0.35$  V, slightly more positive than  $E(2\text{H}^+/\text{H}_2)$ , consistent with the small overpotential for  $\text{H}_2$  oxidation observed for this enzyme.<sup>15</sup> The clear 'switch on' in activity at about  $-0.05$  V during the return sweep towards negative potentials is typical of reductive re-activation of hydrogenases following a reversible inactivation reaction at high potentials which generates the oxidised inactive state known as 'Ready' or Ni-B.<sup>6,15</sup> The enzyme film is fairly stable on the electrode, and the drop in activity on the second cycle (shown in grey) is very slight. However, after removing the electrode, spotting on 0.5  $\mu\text{L}$  of buffer, and replacing the electrode in buffered electrolyte, some loss of current is evident between traces (ii) and (iii), indicating that these manipulations slightly destabilise the film. Traces labelled (iv) were recorded after removing the electrode again, coating it with a layer of Nafion-phosphate, and allowing the layer to dry partially over 5 min, before reinserting it into the same buffered electrolyte. The enzyme film remains electroactive, and the small drop in current, similar to that observed between scans (ii) and (iii), is consistent with slight film destabilisation during application of the overlayer. There is a small drop in current on the second cycle after application of the Nafion-phosphate overlayer (grey trace in (iv)), indicating that the polymer electrolyte does not trap the enzyme at the electrode surface but allows desorbed molecules to escape, presumably into water-filled channels in the polymer structure.

We next determined suitable conditions for assembly of a high surface-area 3-dimensional electrode from hydrogenase-modified carbon particles in Nafion-phosphate. Efficient electron transfer in the film relies upon good mechanical connectivity between particles, but too high a loading of particles compromises the stability of the film. Fig. 4B shows the response at a PGE RDE modified with *E. coli* hydrogenase-modified particles as described in Methods (solid lines). Following enzyme adsorption, the particles were washed in buffer to remove unbound hydrogenase, so the observed catalytic response must arise from enzyme-loaded particles in electronic contact with the planar electrode. The maximum current is now approximately



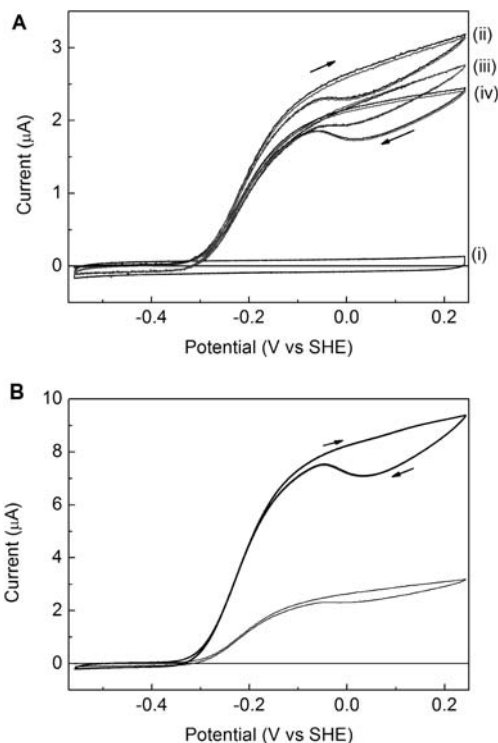


**Fig. 4** Cyclic voltammograms demonstrating that *E. coli* [NiFe]-hydrogenase 1 remains electroactive in contact with Nafion-phosphate, and that a high surface-area electrode can be assembled from enzyme-loaded pyrolytic graphite particles in Nafion-phosphate. Panel A: (i) unmodified pyrolytic graphite 'edge' (PGE) rotating disc electrode (RDE); (ii) PGE RDE modified with a film of *E. coli* [NiFe]-hydrogenase 1; (iii) after removing the electrode used in (ii) from solution, applying a drop of buffer (0.5  $\mu\text{L}$ ) and reinserting into the buffered electrolyte; (iv) after coating the electrode used in (iii) with a layer of Nafion-phosphate (0.5  $\mu\text{L}$ ) and allowing to dry partially for 5 min before reinserting the electrode into the buffered electrolyte. Panel B: PGE RDE modified with a film of hydrogenase-loaded PGE particles applied in Nafion-phosphate binder (thick lines). The trace shown as a thin black line reproduces the first cycle of Panel A (ii). All scans were performed at  $10 \text{ mV s}^{-1}$  in enzyme-free Tris-HCl buffer, pH 8,  $20^\circ\text{C}$  under an atmosphere of  $\text{H}_2$ , with the electrode rotating at 2500 rpm. The PGE surface area of the RDE was  $0.03 \text{ cm}^2$ . In each case, the first cycle is shown in black, and the second cycle is shown in grey. Arrows indicate the direction of scan.

3 times higher than that achieved in the initial scan at a planar electrode (reproduced in this panel as a thin black line), and there is no detectable drop in current between the first and second cycles (the black and grey traces overlay almost completely). Importantly, the shape of the voltammogram is the same as that for hydrogenase directly adsorbed on the planar electrode, and the potentials for onset of catalysis and re-activation are unchanged, indicating that electron transfer to the enzyme is not impaired in the particle film. This result suggests that a high surface-area pyrolytic graphite particle electrode should be suitable for IR spectroscopic studies of hydrogenases and other metalloproteins under direct electrochemical control, providing that sufficient enzyme loading can be achieved.

### Spectroelectrochemistry of ferri/ferrocyanide in a particle-film electrode

In order to test the operation of the ATR-IR cell in a spectroelectrochemical experiment, we used ferricyanide as a convenient test system, incorporated into a particle

film at a loading easily achievable for biomolecules. Ferricyanide does not significantly adsorb onto the surface of pyrolytic graphite particles, but *ca* 1 nmole of  $\text{K}_3[\text{Fe}(\text{CN})_6]$  was incorporated into a Nafion-phosphate particle film. Fig. 5 shows

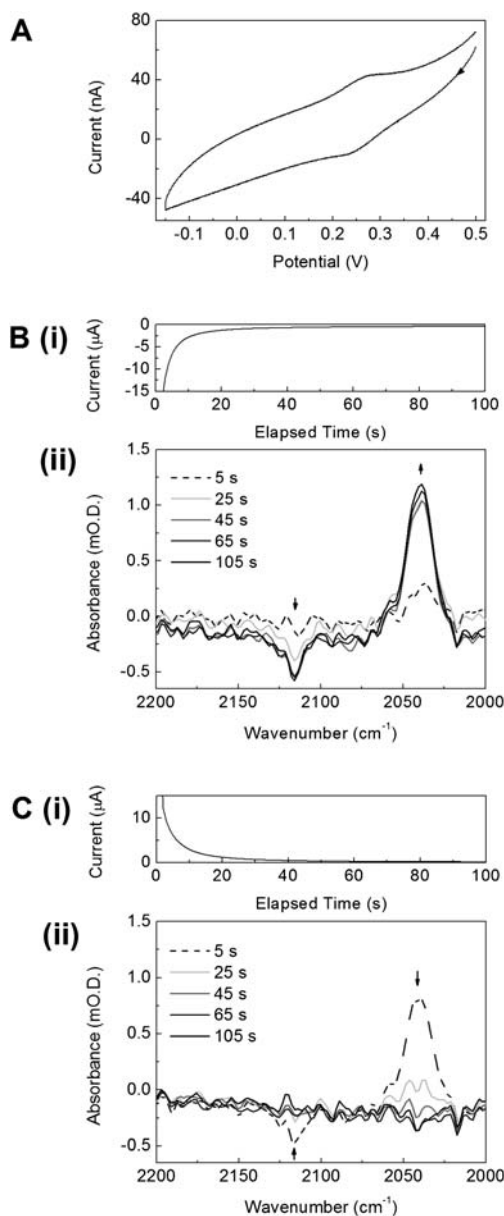


**Fig. 5** Electrochemical and spectroelectrochemical results for a film of  $\text{K}_3\text{Fe}(\text{CN})_6$  (1 nmole) in Nafion-phosphate containing a network of pyrolytic graphite particles in contact with a carbon paper backing plate and gold wire connector in the ATR-IR cell. Spectra represent the average of 16 co-added scans recorded at a resolution of  $4\text{ cm}^{-1}$ . Panel A: Cyclic voltammogram recorded at  $100\text{ mVs}^{-1}$ . Panel B: (i) current-time trace and (ii) ATR-IR difference spectra recorded at the times specified following a potential step from  $+0.4\text{ V}$  to  $-0.2\text{ V}$  vs. the Ag wire pseudo reference electrode. Panel C: (i) current-time trace and (ii) ATR-IR difference spectra recorded at the times specified following a potential step from  $-0.2\text{ V}$  back to  $+0.4\text{ V}$  vs. Ag wire. Spectra are referenced against an initial spectrum recorded at  $+0.4\text{ mV}$ .

results for reduction and re-oxidation of  $[\text{Fe}(\text{CN})_6]^{3-/4-}$  in the spectroelectrochemical cell. Cyclic voltammetric experiments (Fig. 5A) show that reduction and reoxidation are quasi-diffusion controlled, presumably because the ions are able to diffuse in water-filled channels in the Nafion-phosphate structure. Panel B shows the current-time response and accompanying ATR-IR difference spectra recorded following a step from +0.4 V to -0.2 V *versus* the Ag wire pseudo reference electrode. Note that the reference electrode does not hold a stable potential over long time periods, but cyclic voltammetric experiments in the ATR cell confirmed that this potential switch corresponds to stepping over the reduction wave for  $[\text{Fe}(\text{CN})_6]^{3-}$  to generate  $[\text{Fe}(\text{CN})_6]^{4-}$ . The spectra reveal a negative (depletion) band at  $2116\text{ cm}^{-1}$  consistent with loss of the oxidised starting material from the film and a more intense, broad, positive (growth) band at around  $2040\text{ cm}^{-1}$  consistent with formation of  $[\text{Fe}(\text{CN})_6]^{4-}$ .<sup>29</sup> The spectral changes are reversed following a potential step back to +0.4 mV (panel C), indicating that reconversion to the oxidised state is almost complete after 45 s. This is consistent with the decay in current in the chronoamperometric traces, which integrate to give *ca* 0.79 and 0.74 nmoles of electrons passed during this time period for the reduction and re-oxidation steps respectively (ie 79 and 74% conversion within 45 s). Note that since ferricyanide is trapped rather than immobilised in the film, the rate of electrosynthesis is dependent on diffusion and does not reflect a true time constant for electrosynthesis of surface species. Much faster responses following a potential step (<1 s) should be possible for surface adsorbed species.

## Conclusions

In developing an IR spectroelectrochemical approach for studying potential-dependent chemistry of small molecule ligands at metal centres in proteins, we have taken as our starting point the efficient direct electron transfer achieved between many redox proteins and a pyrolytic graphite surface. In particular, protein film electrochemistry has been a powerful tool for controlling and analysing enzymes during fast electrocatalysis, including hydrogenase, nitrite reductase and carbon monoxide dehydrogenase systems which all incorporate or bind ligands with IR-active vibrations.<sup>6,13,22,30</sup> The technical developments we set out in this manuscript describe a strategy for combining IR sampling with direct electrochemical control of proteins on graphite, overcoming the sensitivity challenges of working with low coverage sub-monolayer protein films by exploiting high-surface area electrodes assembled from carbon particles. Electron transfer through the particle films is efficient, giving rise to catalytic voltammograms for immobilised hydrogenase with the same shape as those recorded for enzyme immobilised on a planar electrode (but with higher catalytic currents) and difference spectra for ferricyanide oxidation and reduction.

Although there is often reluctance to handle biological molecules in a solvent or matrix other than water, we show that a Nafion-phosphate polymer electrolyte retains sufficient water to keep enzyme molecules in active conformations. The hydrated polymer matrix of Nafion-phosphate could even be considered more relevant to the *in vivo* environment of proteins in a viscous cellular matrix than studies carried out in dilute solution. Alcohol dehydrogenase was found to be stable in films of Nafion in which protons had been exchanged for tetrabutylammonium ions in an earlier study.<sup>31</sup> In this case the protein, and  $\text{Ru}(\text{bpy})_3^{2+}$  as electron-transfer mediator, were trapped together in the film for electrocatalysis of ethanol oxidation in a fuel cell. A major advantage conferred by Nafion-phosphate as the electrolyte in our studies is its high IR transmittance across most of the mid-IR. This may have particular value in difference spectra involving spectral changes below  $1750\text{ cm}^{-1}$ , for example  $\nu(\text{NO})$  for bound NO, which may otherwise be obscured by the intense water absorption band at  $1700\text{--}1600\text{ cm}^{-1}$  in aqueous solution.

Together the results of this study suggest that application of this ATR-IR strategy to hydrogenases and other redox metalloproteins should be possible. Achieving an

optimal loading of particles in films remains a key challenge, affecting whether the majority of particles are in close physical contact and therefore support efficient electron transfer to adsorbed protein. Film thickness is also critical because optimal electrochemical control is achieved for particles farthest from the prism where IR sampling is less effective due to decay of the IR evanescent wave with distance from the ATR-IR prism. In electrochemical experiments, rapid rotation of the working electrode provides efficient solute mass transport. In the ATR-IR spectroelectrochemical cell, liquid flow could be applied to aid solute mixing. The advances in understanding chemistry at metalloenzyme active sites which are likely to be possible with a surface IR spectroelectrochemical method mean that it is worth establishing strategies to overcome these challenges.

## Acknowledgements

K. A. V. is a Royal Society Research Fellow and an RCUK Academic Fellow and is also grateful to the Royal Society and Jesus College, Oxford for financial support. A. J. H. is grateful for financial support from the OUP John Fell Fund and H. A. R. is grateful for support from Christ Church, Oxford. Staff in the Mechanical Workshops, Department of Chemistry, Oxford University are acknowledged for machining parts for the ATR spectroelectrochemical cell and preparing the CAD diagram of the cell shown in Fig. 2. Dr Robert Jacobs (Oxford University) is thanked for advice on the ATR set-up and initial designs for the cell, and Dr Alison Parkin (also Oxford University) is gratefully acknowledged for providing a sample of *E. coli* hydrogenase 1.

## References

- 1 C. Tard and C. J. Pickett, *Chem. Rev.*, 2009, **109**, 2245–2274.
- 2 S. Groysman and R. H. Holm, *Biochemistry*, 2009, **48**, 2310–2320.
- 3 H. Miyake, T. Okada, G. Samjeské and M. Osawa, *Phys. Chem. Chem. Phys.*, 2008, **10**, 3662–3669.
- 4 J. M. Jin, W. F. Lin and P. A. Christensen, *Phys. Chem. Chem. Phys.*, 2008, **10**, 3774–3783.
- 5 V. D. Colle, A. Berná, G. Tremiliosi-Filho, E. Herrero and J. M. Feliub, *Phys. Chem. Chem. Phys.*, 2008, **10**, 3766–3773.
- 6 K. A. Vincent, A. Parkin and F. A. Armstrong, *Chem. Rev.*, 2007, **107**, 4366–4413.
- 7 F. Armstrong, *Photosynth. Res.*, 2009, **102**, 541–550.
- 8 S. P. Best, S. J. Borg and K. A. Vincent, in *Spectroelectrochemistry*, ed. W. Kaim and A. Klein, Royal Society of Chemistry, 2008.
- 9 S. J. Borg, J. W. Tye, M. B. Hall and S. P. Best, *Inorg. Chem.*, 2007, **46**, 384–394.
- 10 M. H. Cheah, S. J. Borg and S. P. Best, *Inorg. Chem.*, 2007, **46**, 1741–1750.
- 11 A. L. De Lacey, V. M. Fernandez, M. Rousset and R. Cammack, *Chem. Rev.*, 2007, **107**, 4304–4330.
- 12 A. Marechal, Y. Kido, K. Kita, A. L. Moore and P. R. Rich, *J. Biol. Chem.*, 2009, **284**, 31827–31833.
- 13 C. Léger and P. Bertrand, *Chem. Rev.*, 2008, **108**, 2379–2438.
- 14 K. A. Vincent, N. A. Belsey, W. Lubitz and F. A. Armstrong, *J. Am. Chem. Soc.*, 2006, **128**, 7448–7449.
- 15 M. J. Lukey, A. Parkin, M. M. Roessler, B. J. Murphy, J. Harmer, T. Palmer, F. Sargent and F. A. Armstrong, *J. Biol. Chem.*, 2010, **285**, 3928–3938.
- 16 P.-P. Liebgott, F. Leroux, B. Burlat, S. Dementin, C. Baffert, T. Lautier, V. Fourmond, P. Ceccaldi, C. Cavazza, I. Meynial-Salles, P. Soucaille, J. C. Fontecilla-Camps, B. Guigliarelli, P. Bertrand, M. Rousset and C. Léger, *Nat. Chem. Biol.*, 2010, **6**, 63–70.
- 17 K. Ataka and J. Heberle, *J. Am. Chem. Soc.*, 2004, **126**, 9445–9457.
- 18 N. Wisitruangsakul, I. Zebger, K. H. Ly, D. H. Murgida, S. Ekgasit and P. Hildebrandt, *Phys. Chem. Chem. Phys.*, 2008, **10**, 5276–5286.
- 19 D. Millo, M.-E. Pandelia, T. Utesch, N. Wisitruangsakul, M. A. Mroginski, W. Lubitz, P. Hildebrandt and I. Zebger, *J. Phys. Chem. B*, 2009, **113**, 15344–15351.
- 20 N. Wisitruangsakul, O. Lenz, M. Ludwig, B. Friedrich, F. Lenzian, P. Hildebrandt and I. Zebger, *Angew. Chem., Int. Ed.*, 2009, **48**, 611–613.
- 21 T. Reda, C. M. Plugge, N. J. Abram and J. Hirst, *Proc. Natl. Acad. Sci. U. S. A.*, 2008, **105**, 10654–10658.

- 22 J. H. van Wonderen, B. Burlat, D. J. Richardson, M. R. Cheesman and J. N. Butt, *J. Biol. Chem.*, 2008, **283**, 9587–9594.
- 23 K. A. Vincent, X. Li, C. F. Blanford, N. A. Belsey, J. H. Weiner and F. A. Armstrong, *Nat. Chem. Biol.*, 2007, **3**, 761–762.
- 24 O. Lazarus, T. W. Woolerton, A. Parkin, M. J. Lukey, E. Reisner, J. Seravalli, E. Pierce, S. W. Ragsdale, F. Sargent and F. A. Armstrong, *J. Am. Chem. Soc.*, 2009, **131**, 14154–14155.
- 25 L. Xiong and A. Manthiram, *Electrochim. Acta*, 2005, **50**, 3200–3204.
- 26 Y. Kamitaka, S. Tsujimura, N. Setoyama, T. Kajino and K. Kano, *Phys. Chem. Chem. Phys.*, 2007, **9**, 1793–1801.
- 27 Z. Liang, W. Chen, J. Liu, S. Wang, Z. Zhou, W. Li, G. Sun and Q. Xin, *J. Membr. Sci.*, 2004, **233**, 39–44.
- 28 A. Ansari, J. Berendzen, D. Braunstein, B. R. Cowen, H. Frauenfelder, M. K. Hong, I. E. T. Iben, J. B. Johnson, P. Ormos, T. B. Sauke, R. Scholl, A. Schulte, P. J. Steinbach, J. Vittitow and R. D. Young, *Biophys. Chem.*, 1987, **26**, 337–355.
- 29 C. M. Pharr and P. R. Griffiths, *Anal. Chem.*, 1997, **69**, 4665–4672.
- 30 A. Parkin, J. Seravalli, K. A. Vincent, S. W. Ragsdale and F. A. Armstrong, *J. Am. Chem. Soc.*, 2007, **129**, 10328–10329.
- 31 S. Topcagic and S. D. Minter, *Electrochim. Acta*, 2006, **51**, 2168–2172.